Resolution limits for infrared microspectroscopy explored with synchrotron radiation

G. L. Carr[a)]
National Synchrotron Light Source, Brookhaven National Laboratory, Upton, New York 11973

(Received 16 May 2000; accepted for publication 10 December 2000)

The spatial resolution for infrared microspectroscopy is investigated to determine the practical limits imposed by diffraction or optical aberrations. Quantitative results are obtained using high brightness synchrotron radiation, which serves as a diffraction-limited infrared ''point source'' for the microscope. The measured resolving power is in good agreement with diffraction theory, including a ~ 30% improvement for a confocal optical arrangement. The diffraction calculation also shows how the confocal setup leads to better image contrast. The full width at half maximum of the instrument's resolution pattern is approximately $\lambda/2$ for this arrangement. One achieves this diffraction limit when the instrument's apertures define a region having dimensions equal to the wavelength of interest. While commercial microspectrometers are well corrected for optical aberrations (allowing diffraction-limited results), the standard substrates used for supporting specimens introduce chromatic aberrations. An analysis of this aberration is also presented, and correction methods described.

I. INTRODUCTION

Infrared microspectroscopy traces its origins to around 1950 when microscopes using Schwarzschild-type reflecting objectives were interfaced to infrared monochromators.[1] The technique languished due to the poor efficiencies of spectrometers until the 1980s when Fourier transform infrared (FTIR) spectrometers became commercially available. Present day FTIR spectrometers and microscopes are well matched and deliver high performance. Still, signal-to-noise requirements (e.g., for identifying small chemical changes) often limit the smallest practical spotsize to ~20 μm. This is a consequence of the low brightness of the thermal infrared source (a~1200 K blackbody radiator) rather than diffraction or aberrations in the optical system.

High brightness infrared sources do exist (e.g., lasers), but of these only the synchrotron[2] provides a ''white'' source spanning the entire infrared and is compatible with efficient FTIR techniques. While early attempts to exploit this as an infrared source were unsuccessful due to poor beam stability, the present generation of synchrotron light sources have overcome this problem to a large extent and productive infrared research programs now exist at a number of facilities. The National Synchrotron Light Source (NSLS) at Brookhaven National Laboratory has six operating infrared ''ports,'' several of which deliver infrared to microspectrometers.[3] The high brightness of this source (two to three orders of magnitude greater than conventional thermal sources) allows one to set the instrument's apertures to define geometrical areas comparable to, or smaller than, the diffraction limit (a few microns in the midinfrared) and still attain good signal to noise (S/N).[4–6] For this situation, the spatial resolution is no longer controlled by the geometrical aperture size, but instead is determined by the optical system's numerical aperture and the wavelength of light.

While the microscope's optical system performs at or close to the diffraction limit for the spectral range of interest, on occasion the specimen to be studied introduces aberrations that limit the available spatial resolution. A common sample preparation method involves placing thin sections onto IR transparent substrates. However, the substrate materials are typically dispersive and therefore introduce chromatic aberration. The resulting focus shifts can be comparable to, or larger than, the region under investigation. This leads to a reduction in spatial resolution, signal throughput, or both.

In this article an analysis of a typical infrared microscope optical system is presented and practical issues for achieving diffraction-limited performance are addressed. The first part deals with experimental results and calculations for the instrument's spatial resolution (i.e., the sensitivity pattern). Agreement between the two is good and a confocal optical system is found to reduce (improve) the width of the instrument's sensitivity pattern by about 30% over the single-aperture case. Of perhaps greater importance, the confocal system reduces contributions from the first- and higher-order diffraction maxima (diffraction rings) which otherwise would degrade spatial contrast. The dependence of the sensitivity pattern width on aperture dimension is discussed in Sec. II. It is found that an aperture size equal to the wavelength of light achieves the diffraction limit. Last, the focus shift associated with dispersive substrates is calculated for a number of substrate materials. Focus shifts of up to 100 μm occur when using 2 mm thick BaF_2 at wavelengths of 10 μm. The results of experiment and calculation are again in good agreement.

a)Electronic mail: carr@bnl.gov

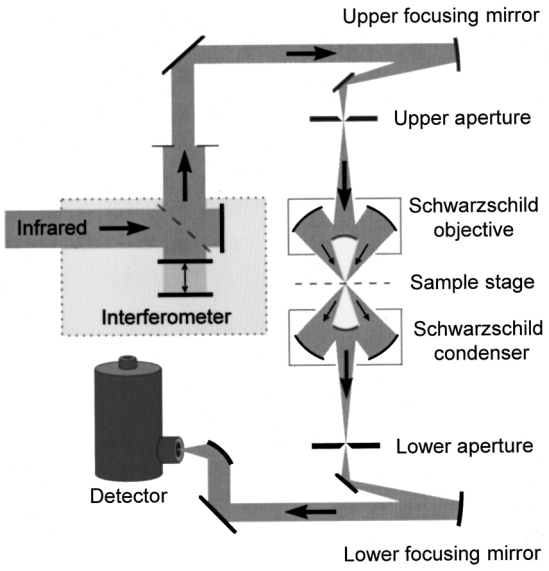

FIG. 1. Schematic diagram of the infrared microspectrometer (a Spectra-Tech *Ir* μs™) used for this study. The optical path for transmission (shown in the diagram) begins at the FTIR interferometer and continues through the upper aperture, the first Schwarzschild objective, the sample/specimen, the Second Schwarzschild objective (often refered to as a condenser), the lower aperture, and finally to the detector. For a reflection measurement, the light reflected by the sample returns backward through the first Schwarzschild objective and upper aperture, after which a small ''pick-off'' mirror intercepts a portion of the light and sends it on to the detector.

II. EXPERIMENT AND ANALYSIS

A. Instrumentation

The spectral range commonly employed for analytical infrared microscopy is from 4000 ($\lambda = 2.5\,\mu$m) down to 650 cm^{-1}($\lambda = 16\,\mu$m). The wavelengths are therefore 5–10 times greater than for visible light, and microscope optical designs can be readily fabricated to achieve the diffraction limit. The particular microspectrometer used for this study is a Spectra-Tech *Ir*μ*s*.[7] It has a confocal optical system based on two Schwarzschild objectives, each having a numerical aperture (NA) of about 0.65. The specimen to be studied is placed at their common focus. Spatial resolution is achieved by field stops (apertures) located at one or both conjugate focal points of the objectives. One aperture controls the region being illuminated while the other defines the region being sensed by the IR detector. A schematic of this instrument's optical system is shown in Fig. 1.

This microscope's objectives differ from a true Schwarzschild type in that both conjugates are finite, and therefore do not fully correct for typical aberrations (e.g., spherical one). However, optical analysis using ZEMAX™ optical analysis software[8] shows that they do achieve diffraction-limited performance across the midinfrared, and image quality at visible wavelengths implies a resolution of better than 1 μm on axis. Since the objectives are all reflecting, chromatic aberrations are not present.

Although the optical system is capable of diffraction-limited performance, the standard source for mid-IR spectroscopy (a 1200 K thermal source) is not typically bright enough to provide the necessary S/N when the diffraction limit is reached. Infrared produced as synchrotron radiation is substantially brighter (two to three orders of magnitude) and provides good S/N even when the microscope's apertures are set at, or beyond, the diffraction limit. In this situation, the wavelength and the system's numerical aperture determine the spatial sensitivity. The measurements described here were performed with the instrument installed at the U10B infrared beamline[5] of the NSLS.

B. Spatial resolution and diffraction

A microscope achieves spatial resolution by constraining the illuminated region, the region being detected, or (more generally) a combination of both. For example, a standard optical microscope illuminates a large sample region and resolution is achieved by the ''detection system,'' in this case the objective optics and receptors in the eye. A microscope using a focal-plane detector is a similar case in which resolution is attained from the individual pixels of the optical detection system. One can also use a single element detector and restrict the field of view at the sample location by an aperture placed at an intermediate focal point (a field stop). The spatial resolution is determined by the detection sensitivity pattern $D(\boldsymbol{r})$, defined as the fraction of light from each point $\boldsymbol{r}$ of the specimen that reaches the detector. Alternatively, one can restrict the illumination region (again using an aperture that serves as a field stop) to achieve spatial resolution. Here the resolution is determined by the pattern of illumination $I(\boldsymbol{r})$ defined as the fraction of light intensity illuminating each point on the specimen. A confocal microscope has apertures for both the illumination and detection systems, constraining both patterns (I and D). To sense a particular portion of a specimen, the microscope must illuminate it and then detect that light. Thus for linear spectroscopy, the spatial sensitivity ''pattern'' of the instrument $S(\boldsymbol{r})$ is determined by the product $I(\boldsymbol{r}) \times D(\boldsymbol{r})$. An image of the specimen can be ''built up'' by rastering the sample through the instrument's illumination and detection pattern. Such an image is the convolution of this sensitivity pattern with the true specimen image. Thus the product $S \equiv I \times D$ determines the spatial resolution.

When aberrations are negligible and the microscope aperture(s) is set to define a geometric region smaller than the wavelength, diffraction dominates the sensitivity pattern and consequently the spatial resolution of the instrument. Further reduction of the apertures offers no resolution improvement. If the illumination and detection objectives behave as simple lenses with the same NA, then $I(\boldsymbol{r})$ and $D(\boldsymbol{r})$ would each be described by the same Airy function. Note that the product of two identical Airy functions is narrower than the individual functions by about 30%. In addition, the contributions of the first- and higher-order diffraction maxima (relative to the central, zero-order maxima) are significantly reduced. This illustrates how a confocal microscope achieves higher spatial resolution when diffraction-limited conditions exist.

C. Measurements

The instrument's lateral sensitivity was determined by scanning across a lithographically produced photoresist step edge and measuring the apparent sharpness at various wave-

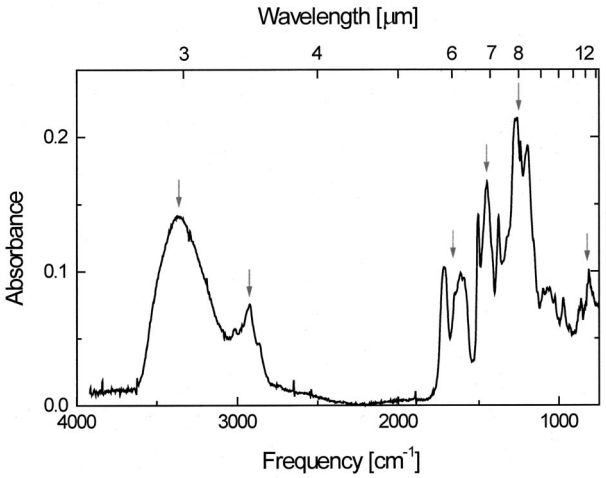

FIG. 2. Absorbance spectrum for the photoresist material used for resolution studies. The six absorption features used for the profile analysis are marked with arrows.

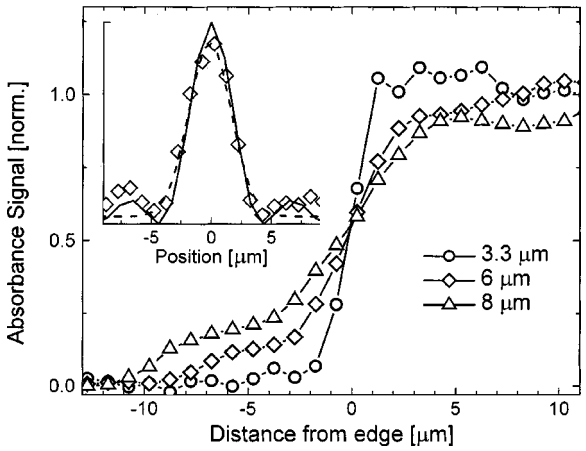

FIG. 3. Absorbance profiles at three different wavelengths acquired at 1 μm intervals across a photoresist step edge. Inset: Deconvolution of the profile for $\lambda = 6$ μm, revealing the illumination pattern $I(x)$.

lengths. The photoresist layer was approximately 2 μm thick, and the edge ''sharpness'' was better than 1 μm. Its absorbance spectrum, shown in Fig. 2, displays vibrational features spanning the spectral range from 3 to 12 μm wavelengths ($\sim$3300 down to 830 cm^{-1}). The substrate was either BaF_2 (appropriate for transmission measurements) or a gold mirror (for reflectance).

The first type of resolution test was performed using only the instrument's ''upper'' field stop aperture to constrain I (see Fig. 1). For simplicity, the spatial sensitivity was investigated only along one direction by setting the upper field stop to a slit 32 μm wide and about 1 mm long. When used with the 32$\times$ objective, the resulting effective aperture width is 1 μm at the specimen location, which is smaller than the shortest wavelength of interest by a factor of 3. The actual illumination pattern is more or less independent of position along the slit and dominated by diffraction transverse to the slit. The resolution tests were conducted for this transverse direction. No aperture was used for the detection optical system. Thus the system was not confocal for this set of measurements (the confocal case is treated later).

Transmission spectra were collected at 1 μm intervals along a line, beginning 15 μm before the edge and continuing 15 μm into the photoresist. From these, absorbance profiles for spectral bands at various wavelengths were extracted. Selected profiles for absorbance features at 3, 6, and 8 μm wavelengths are shown in Fig. 3. Although the photoresist edge is sharp, the profiles are broadened in all cases, with the degree of broadening increasing with wavelength as expected from diffraction. Similar results have been reported by Ocola *et al.*[6] As noted above, the measured profile is a convolution of the illumination function I with the actual edge profile. Assuming the edge is perfectly abrupt, one can deconvolve the data to produce the pattern of illumination transverse to the narrow slit aperture, in this case $I(x)$. The illumination pattern that results for $\lambda = 6$ μm is shown in the inset of Fig. 3 (symbols). A convenient method for extracting the width of the pattern's central maximum is to fit it with a Gaussian function. Such a fit is also shown in the inset.

A second set of measurements was performed with apertures constraining both the illumination and detection patterns, i.e., a confocal optical arrangement. Although the microscope system can perform transmission measurements in confocal mode (using both upper and lower apertures, or double aperturing), it was convenient to use the microscope in reflectance mode where the same objective and aperture are used for illuminating the specimen and collecting the reflected light for detection. Reflectance measurements were made using an identical (to the transmission case) photoresist step edge deposited on a gold substrate. Absorbance profiles were extracted and deconvolved in the same manner as for the transmission measurement. The resulting resolution widths for the six different absorption features are shown in Fig. 4 (symbols), plotted versus their respective wavelength. Results for both the single and confocal optical arrangements are included. Note that the error bars are much larger here than for the single aperture case due to the rather poor signal to noise, a consequence of the infrared light having passed

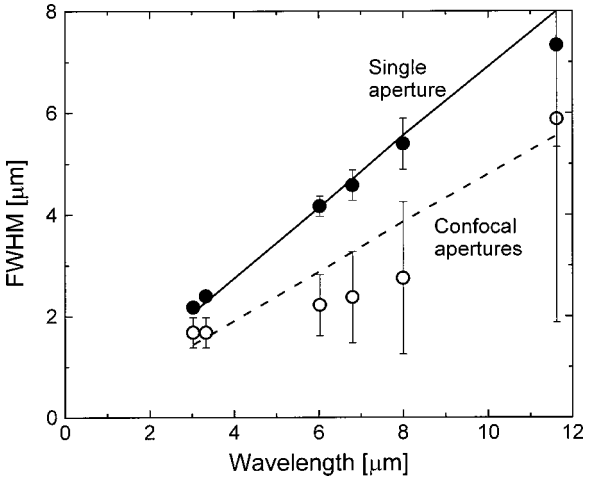

FIG. 4. FWHM for the resolved photoresist edge profile. Closed circles: Single aperture; open circles: dual (confocal) apertures; solid line: calculated PSF width for one apertures; dashed line: calculated PSF for confocal apertures.

twice through the aperture (which has a dimension much smaller than the wavelengths of interest).

D. Model calculations

In addition to measuring the microscope's spatial resolving power, the point spread function (PSF) for the illumination objective was calculated using ZEMAX optical design/analysis software running on a personal computer. Note that the PSF and diffraction pattern are equivalent when aberrations are negligible. As a consequence of the objective's secondary mirror obscuration, the PSF involves a linear combination of two Bessel functions. The effect of this combination is to narrow the central (zero-order) peak while enhancing the magnitude of the first- and other higher-order diffraction maxima. Since the calculation was performed for just the illumination objective, this PSF gives the expected sensitivity pattern I for a single aperture measurement. The PSF is shown in the inset of Fig. 3 for $\lambda = 6\ \mu$m, along with the measured result for I and a Gaussian fit. Although the calculation considers only a point source (whereas the measurement determined the diffraction pattern transverse to a line source), agreement is very good, including the location and magnitude of the first-order diffraction maxima. Thus the illumination pattern I is well described by the PSF under diffraction-limited conditions, as expected. The PSF was also fit with a Gaussian (for consistency) and the full width at half maximum (FWHM) for both the measured pattern I (closed circles) and the diffraction PSF (solid line) are plotted versus wavelength (see Fig. 4). The FWHM of the illumination pattern I is found to be approximately $2\lambda/3$.

We expect the confocal case to have a sensitivity pattern given by the product of $I \times D$. Since the same objective and aperture were used for both I and D, the sensitivity pattern will be I^2. Squaring the PSF produces a pattern ~30% narrower, yielding a FWHM of $\sim\lambda/2$. The results, shown in Fig. 4 (dashed line), are again in reasonable agreement with the experiment (open circles) when one takes into account the large error bars for the experimental data.

The confocal optical arrangement provides another important benefit over a single optic system. Figures 5 and 6 show a two-dimensional view of the PSF for a conventional optic with a circular aperture (Fig. 5) and a Schwarzschild optic having a circular obscuration centered in the aperture (Fig. 6). For the latter, the radius of the obscuration was taken to be one half the overall aperture, thus allowing 75% of the incident light to pass (a reasonable value). The increased intensity in the higher-order diffraction maxima is evident, and represents a substantial fraction of the overall intensity. This can be better illustrated by calculating the weighted sensitivity enclosed within circular regions, centered on the optical axis, as a function of the circle's radius [see Figs. 5(b) and 6(b)]. The standard optic yields an Airy pattern with about 85% of the total sensitivity contained within the zero-order peak, whereas the Schwarzschild diffraction pattern has only ~50% of the total sensitivity near the center. With half the sensitivity contained outside the central peak, the Schwarzschild objective is subject to serious degradation of image contrast when used for scanning

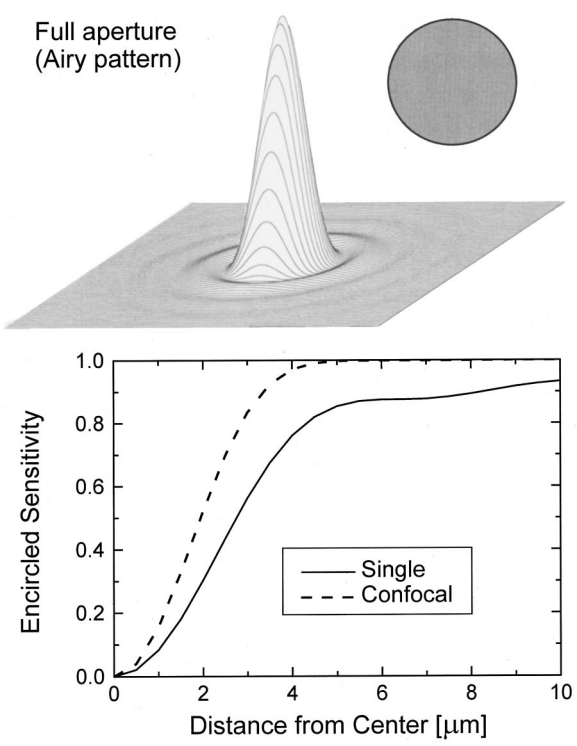

FIG. 5. Top: The point spread function (diffraction pattern) for an optic having a full circular aperture (indicated by the gray area in the inset, upper right). A wavelength of 6 μm and an optical NA of 0.6 were assumed. This is the familiar Airy pattern. Bottom: The encircled sensitivity as a function of radial distance from the center point (optic axis) for a system with full circular apertures. Note that the confocal arrangement maintains more than 90% of the sensitivity to within 3 μm of the central axis.

microscopy. The confocal arrangement improves the situation substantially, with 80% of the spatial sensitivity contained within the primary, zero-order peak. Thus the confocal system should allow better isolation of small regions (with much less contamination from neighboring regions) and improved contrast in scanned or imaging measurements. This is perhaps the most important benefit of the confocal optical arrangement. Since infrared microspectrometers using array detectors or cameras are not confocal, one should not expect them to achieve the same level of diffraction-limited performance.

E. Dependence on aperture dimensions

Finally, a crossover from a diffraction (wavelength) limited resolution to a geometrically controlled resolution must occur as the aperture width is increased. This crossover can be predicted by convolving the PSF (diffraction pattern) with the geometrical aperture shape. Such a calculation was performed for $\lambda = 8\ \mu$m and geometric aperture dimensions up to 12 μm, with the FWHM determined for each aperture setting. In the same manner as for the resolution patterns described above, the FWHM for various actual aperture widths was extracted from absorbance measurements across the photoresist edge. Both the calculated (dashed line) and measured (closed circles) widths are shown in Fig. 7. The calculated width begins to curve upwards (with increasing aperture width) almost immediately, whereas the measured width remains near the diffraction-limited minimum until the

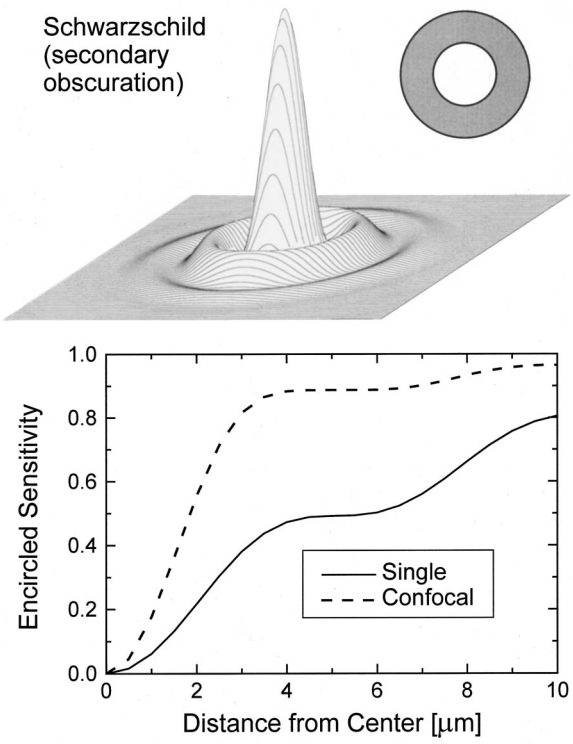

FIG. 6. Top: The point spread function (diffraction pattern) for an optic with a secondary mirror (central) obscuration. The aperture is indicated by the gray area in the inset, upper right. A wavelength of 6 μm and an optical NA of 0.6 were assumed. Note the enhanced size of the first-and higher-order diffraction ''rings.'' Bottom: The encircled sensitivity as a function of radial distance from the center point (optic axis) for a Schwarzschild objective. Note that the conventional arrangement (single objective) has only 50% of the sensitivity within the central diffraction maximum, and reaches 80% only at a 10 μm radial distance. The confocal arrangement manages to narrow the central maxima and also achieves 90% sensitivity within a 4 μm radius.

aperture is nearly equal to the wavelength. This discrepancy may be explained as a consequence of how electromagnetic radiation propagates through the field-defining aperture, which behaves as a short length of waveguide.[9] Until the aperture is wide enough to support more than the fundamental mode (i.e., width $\geqslant\lambda$), the light appears to emanate from

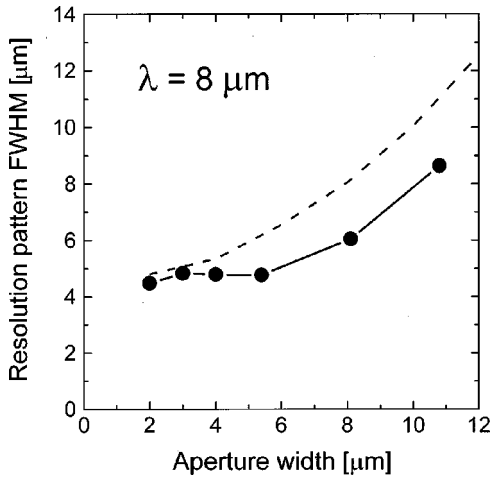

FIG. 7. FWHM (resolution width) as a function of aperture width for a single aperture and $\lambda = 8$ μm.

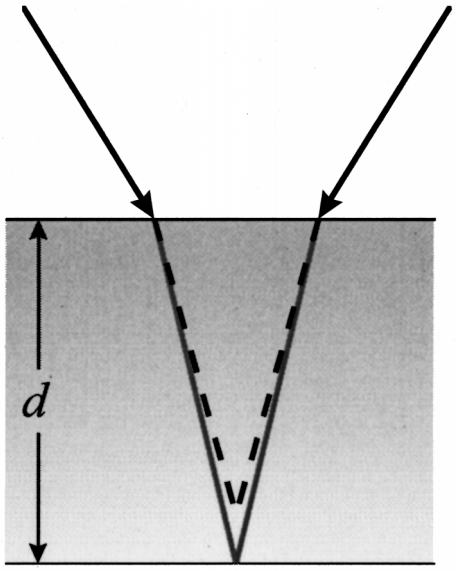

FIG. 8. Illustration of the focus shift that occurs for dispersive substrates.

a diffraction-limited region that is independent of the actual width. Thus, decreasing the aperture size to below 8 μm yields no gain in spatial resolution when profiling an absorbance feature near 1250 cm^{-1}. Since the signal to noise falls rapidly as the apertures are closed further, a size essentially equal to the wavelength of interest is probably optimal. Thus, the signal to noise for the sensitivity pattern tests of Fig. 4 could be dramatically improved at longer wavelengths by opening the apertures, while still attaining diffraction-limited performance. Additional improvements in spatial resolution may be achieved by oversampling and deconvolving the instrument's PSF. Other approaches include increasing the NA with high refractive index materials, or near-field methods.[10]

F. Substrate dispersion

The diffraction-limited performance demonstrated in Sec. II E is attained only when the optical system's aberrations are sufficiently small. The microscope's basic optical system clearly reaches this goal. However, a specimen to be studied may require a supporting substrate, or might be contained between two infrared windows. The substrate becomes part of the optical system when the infrared light passes through it, and any aberrations introduced must be addressed. Adjusting the spacing of the two mirror elements for the relevant Schwarszchild objective adequately eliminates the spherical aberration that results, and the microscope manufacturer provides for this adjustment. But chromatic aberration cannot be readily corrected, and is compounded by the large spectral range that is desired for most analytical measurements.

Chromatic aberration is due to the dispersive properties of materials and gives rise to focus shifts between wavelengths. An illustration of this effect is shown in Fig. 8 where polychromatic light is incident on a substrate of thickness *d*. Whereas one wavelength comes to a focus at the back surface, another (typically longer) wavelength comes to a focus within the substrate (before reaching the back surface). Of

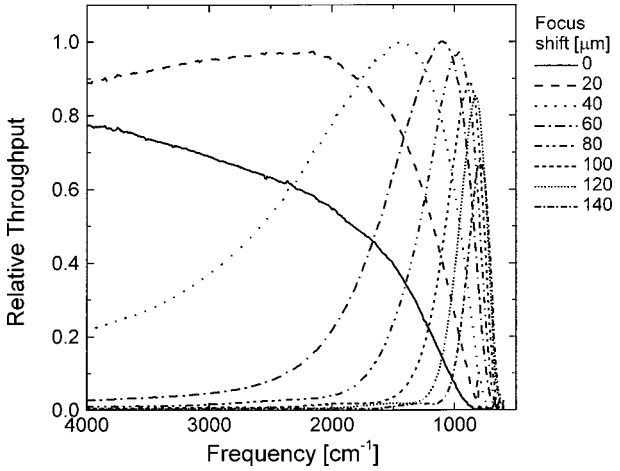

FIG. 9. Relative transmission through a 2 mm thick BaF_2 substrate at various focus settings.

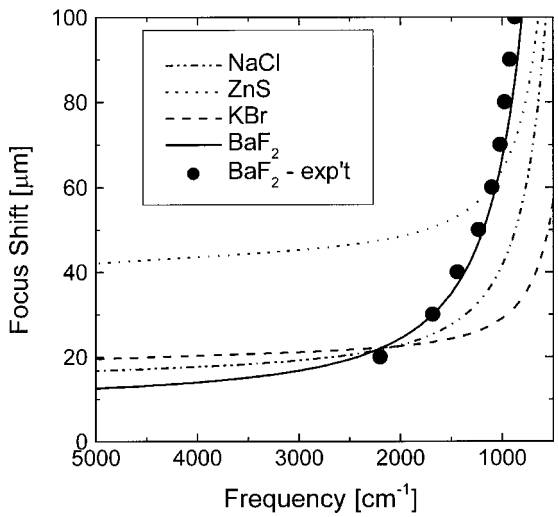

FIG. 10. Lines: Calculated focus shift for several common IR substrate materials (all 2 mm thick), including BaF_2. Closed circles: Measured focus shift for BaF_2.

course any particular wavelength can be brought into proper focus by shifting the substrate, but at the expense of others.

The effect can be readily shown for a commonly used substrate, a 2mm thick BaF_2 wafer. The microscope's apertures (both upper and lower) were set to about $5\,\mu$m $\times 5\,\mu$m and a background spectrum was collected with no substrate. Next, the BaF_2 substrate was placed at the specimen location of the $Ir\mu s$ microspectrometer and both upper and lower objectives set for proper visual focus on the same substrate surface. Naturally, one of the objectives must be focused through the substrate, making it sensitive to the substrate's dispersion. For convenience of measurement, the upper (illuminating) objective was focused through to the far surface of the BaF_2 substrate. Shifting the focus position for this objective (by an amount defined as f_{shift}) brings various wavelengths into proper focus on the far surface of the substrate. The spectral signal through the BaF_2 was measured and normalized to the background signal (i.e., no substrate present) to yield the apparent transmission. Measurements for various f_{shift} values ranging from 0 to 160 μm were acquired at 10 μm increments. The zero position was defined as the position at which the substrate surface was visually focused. The apparent transmission for every other position (i.e., at 20 μm intervals) is shown in Fig. 9. Note that for $f_{\text{shift}}=0$, the infrared throughput is reduced across the entire IR spectral range, and falls rapidly for wavelengths $\sim 10\,\mu$m. This reduction far exceeds absorption or reflectance losses at the air/BaF_2 interfaces. A 20 μm focus adjustment increases the throughput at all mid-IR wavelengths, with 2200 cm^{-1} being optimal. Additional shifting of the focus improves the throughput for longer wavelengths, but at the expense of shorter ones. The signal maximum (peak throughput) indicates the frequency that is properly focused when substrate absorption is negligible.

The amount of shift needed to bring a particular wavelength into focus can be calculated using Snell's law. The resulting approximate expression is

$$f_{\text{shift}} \approx \frac{d}{n_0}\left(1-\frac{n(\lambda)}{n_0}\right), \tag{1}$$

where d is the substrate thickness, $n(\lambda)$ is the material's refractive index at wavelength λ, and n_0 is the refractive index at some reference wavelength (in our case, a visible wavelength such as 570 nm). The calculated focus shifts for 2 mm thick BaF_2 and other common materials[11] are shown in Fig. 10. Also shown is the experimentally determined focus shift versus the peak transmission frequency for the BaF_2. Agreement between the calculation and measurement is very good, although less so toward longer wavelengths. This is probably a consequence of the BaF_2 absorption, which causes the apparent transmission to turn downwards more quickly than from focus errors alone. Thus, the position for optimal focus for an absorbing substrate may not be precisely where the throughput is maximized. The magnitude of the focus shift is particularly noteworthy, becoming more than 20 times the intended illumination size, leading to a comparable reduction in spatial resolution.

As can be seen in Fig. 10, the problem is not limited to BaF_2. While KBr has less dispersion at long wavelengths, there is more dispersion in the visible. The result is that a focus optimized for visible wavelengths is 20 μm out of focus across the entire mid-IR.

Since the magnitude of the focus error scales linearly with thickness, the problem can be reduced by the use of thinner substrates. This may eventually lead to problems from interference fringes due to multiple internal reflections within the substrate. Another approach that partially avoids the problem is to place the specimen on top of the substrate and use only the upper illumination aperture to achieve the desired spatial resolution. The beam converges at the sample (and before the substrate), so all wavelengths come to the same focus. The collecting objective is then set for an intermediate focus setting, and its conjugate aperture is left open. Thus the collecting optics are rather insensitive to focus errors. Of course one loses the benefits of a confocal optical system, resulting in poorer resolution and image contrast. In an imaging IR microspectrometer (with a focal plane array detector or camera), each detector pixel serves as a field-

defining aperture. Spatial resolution is therefore achieved only through the detection system (i.e., it is not confocal). The sample side of the substrate should be oriented facing the detector for these systems.

There are cases where this problem cannot be avoided, for example, samples sandwiched between two substrates as in a liquid or compression cell, or when the instrument must be operated in a true confocal mode. In order to achieve optimal spatial resolution, the measurement must be repeated for each wavelength range of interest, adjusting the instrument's focus to match the spectral range. The focus error that can be tolerated depends on the measurement, but should be smaller than the wavelength if diffraction-limited performance is to be attained. For BaF_2, this becomes increasingly problematic for longer wavelengths, and it may be impossible to have even a single absorption band entirely in focus. As an example, the relative focus shift across a 200 cm^{-1} wide band near 1000 cm^{-1} ($\lambda = 10\ \mu m$) is more than 20 μm, exceeding the wavelength by a factor of 2.

ACKNOWLEDGMENTS

Useful conversations with J. Reffner (SensIR, Inc.), D. Schiering, T. Tague (Spectra-Tech, Inc.), P. Dumas (LURE/CNRS), L. M. Miller (NSLS), and L. Richter (NIST) are gratefully acknowledged. L. M. Miller assisted with some of the measurements, and P. Dumas provided a critical reading of the manuscript. The photoresist patterns used for the resolution tests were supplied by Spectra-Tech. This work was supported by the U.S. Department of Energy through Contract No. DE-AC02-98-CH10886 at the NSLS. The U10B beamline and *Ir*μs™ microspectrometer are operated by the NSLS and the Northrop Grumman Corporation. The NSLS operates as a User Facility, open to all qualified researchers. Information can be found at http://www.nsls.bnl.gov and http://infrared.nsls.bnl.gov.

[1] R. Barer, A. R. H. Cole, and H. W. Thompson, Nature (London) **163**, 198 (1949).
[2] W. D. Duncan and G. P. Williams, Appl. Opt. **22**, 2914 (1983).
[3] G. L. Carr, P. Dumas, C. J. Hirschmugl, and G. P. Williams, Nuovo Cimento D **20**, 375 (1998).
[4] J. A. Reffner, P. Martoglio, and G. P. Williams, Rev. Sci. Instrum. **66**, 1246 (1995); G. L. Carr, J. A. Reffner, and G. P. Williams, *ibid.* **66**, 1490 (1995).
[5] G. L. Carr, O. Merlo, M. Munsli, S. Springer, and S. C. Ho, Proc. SPIE **3775**, 22 (1999).
[6] L. E. Ocala, F. Cerrina, and T. May, Appl. Phys. Lett. **71**, 847 (1997).
[7] *Ir* μs™ scanning infrared microspectrometer, Spectra-Tech Inc., Shelton, CT.
[8] ZEMAX software, Focus-software, Inc.
[9] See, for example, J. D. Jackson, *Classical Electrodynamics* (Wiley, New York, 1976), Chap. 8.
[10] See, for example, M. Ohtsu and H. Hori, *Near-field Nanooptics* (Kluwer Academic, Plenum, New York, 1999).
[11] *Handbook of Optical Constants of Solids II*, edited by E. D. Palik (Academic, Orlando, FL, 1991), pp. 177–201.